Eur. Phys. J. B **44**, 415–421 (2005)
DOI: 10.1140/epjb/e2005-00140-5

THE EUROPEAN PHYSICAL JOURNAL B

# Signatures of polaron formation in systems with local and non-local electron-phonon couplings

E. Piegari[1], C.A. Perroni[1,2], and V. Cataudella[1,2,a]

[1] Dipartimento di Scienze Fisiche, Universitá di Napoli "Federico II", via Cinthia 80126 Napoli, Italy
[2] Coherentia-INFM, UdR di Napoli, via Cinthia 80126 Napoli, Italy

Received 23 December 2004
Published online 30 May 2005 – 

**Abstract.** Polaron formation is investigated in a one-dimensional chain by taking into account both the local Holstein and the non-local SSH electron-phonon interactions. The study of the adiabatic regime points out that the combined effects of the two interactions are important mainly in the weak coupling regime. Thus, using the weak-coupling perturbation theory, spectral weights, effective masses, polaronic phase-diagram, and band structures are discussed. Contrarily to what happens in the Fröhlich and Holstein models, we find that the ratio between the coherent spectral weight and the mass renormalization ratio is greater than 1. Moreover, we show that the non-local electron-phonon interaction is responsible for the largest deviations of the band structure from the cosine shape of the free energy band.

**PACS.** 71.38.-k Polarons and electron-phonon interactions

## 1 Introduction

In the last years the presence of relevant electron-phonon (el-ph) interactions and polaron signatures [1,2] has been evidenced in several compounds, like manganites [3], fullerenes [4], carbon nanotubes [5,6], cuprates [7], DNA and conducting polymers [8–12]. The amount of experimental data has intensified the study of realistic lattice interaction models, stimulating the interest for those where the effects of more complex electron-phonon couplings are taken into account [12].

In this paper we study the Hamiltonian that has been derived from general arguments for an electron-harmonic lattice system, under the only assumption that the electronic transfer integral and the electronic local energy are linear functions of the lattice displacements [13]. According to this analysis a single electron interacts with an optical phonon mode through both the local Holstein coupling [14] and the non-local SSH (Su-Schrieffer-Heeger) coupling [15]. We notice that this non-local SSH coupling differs from the conventional one where acoustical, instead of optical, phonons are considered [15]. Since the electronic transfer integral typically depends on the lattice displacements, the model can be used to describe different systems with different relative importance of the two el-ph interactions.

A preliminar perturbative analysis of the proposed model is contained in reference [13], where the ground state properties have been characterized evaluating the ground state energy, the electron-lattice correlation functions, the phonon number and the spectral weight. However, in reference [13] the attention focuses only on the non-local limit.

Our purpose in this paper is to examine how the two different Holstein and SSH el-ph interactions simultaneously affect the polaronic state. In Section 2 we present the model. In Section 3 we study the adiabatic regime showing that in this limit, characterized by the neglecting of the quantum lattice fluctuations, the effects of the combined interactions are important only for weak coupling. Thus, in Section 4, using the weak-coupling perturbation theory, we analyze the behaviors of the spectral weight and the polaron effective mass as functions of the two el-ph coupling constants and the adiabaticity ratio. The pertubative results clearly show that the electron undergoes a mass enhancement larger than the reduction of the spectral weight, pointing out the relevance of the non-local el-ph coupling for the tendency towards localization. Moreover, according to the values assumed by the spectral weight, a phase diagram is presented in order to locate the region of the coupling values where a crossover regime begins. Finally, we study the band structure as function of the el-ph coupling constants and the adiabaticity ratio, showing that the major contribution to the renormalized electron band comes from the non-local coupling. Conclusions are summarized in Section 5.

[a] e-mail: vittorio.cataudella@na.infn.it

## 2 The model

The real space Hamiltonian which describes electrons in interaction with harmonic lattice deformations [13] reads

$$\mathcal{H} = \sum_{i,j,\sigma} c^{\dagger}_{i,\sigma} t_{i,j}(\{x_k\}) c_{j,\sigma} + \sum_i \frac{p_i^2}{2M} + \sum_{i,j} \frac{x_i K_{i,j} x_j}{2} + \sum_{i,\sigma} e_i\left(\{x_k\}\right) c^{\dagger}_{i,\sigma} c_{i,\sigma}, \quad (1)$$

where $c^{\dagger}_{i,\sigma}$ ($c_{i,\sigma}$) is the fermion creation (destruction) operator, $\sigma$ is the spin index, $t_{i,j}(\{x_k\})$ is the electronic transfer integral for fixed lattice deformations $\{x_k\}$, $M$ is the ionic mass, $K_{i,j}$ is the spring constant matrix, and $e_i(\{x_k\})$ is the local energy of the electron. Limiting the hopping to nearest-neighbor sites of a linear chain, we consider that $t_{i,j}(\{x_k\})$ and $e_i(\{x_k\})$ are linear functions of the lattice displacements $\{x_k\}$

$$t_{n+1,n}\left(\{x_k\}\right) = -t + \alpha_{ssh}(x_{n+1} - x_n), \quad (2)$$

$$e_i(\{x_k\}) = \alpha_{hol} x_i. \quad (3)$$

Thus for spinless electrons and dispersionless Einstein phonons the Hamiltonian can be written as

$$\mathcal{H} = -t \sum_i \left( c^{\dagger}_i c_{i+1} + c^{\dagger}_{i+1} c_i \right) + \sum_i \left[ \frac{p_i^2}{2M} + \frac{1}{2} K x_i^2 \right] + \mathcal{H}_{int}, \quad (4)$$

with

$$\mathcal{H}_{int} = \alpha_{ssh} \sum_i \left( c^{\dagger}_i c_{i+1} + c^{\dagger}_{i+1} c_i \right) (x_{i+1} - x_i) + \alpha_{hol} \sum_i x_i c^{\dagger}_i c_i. \quad (5)$$

Using the second quantization for phonon operators, the Hamiltonian becomes

$$\hat{H} = -t \sum_i \left( c^{\dagger}_i c_{i+1} + c^{\dagger}_{i+1} c_i \right) + \omega_0 \sum_i \left[ a^{\dagger}_i a_i + \frac{1}{2} \right] + \hat{H}_{int}, \quad (6)$$

with

$$\hat{H}_{int} = g_{ssh} \omega_0 \sum_i \left( c^{\dagger}_i c_{i+1} + c^{\dagger}_{i+1} c_i \right) \times \left( a^{\dagger}_{i+1} + a_{i+1} - a^{\dagger}_i - a_i \right) + g_{hol} \omega_0 \sum_i c^{\dagger}_i c_i (a^{\dagger}_i + a_i), \quad (7)$$

where $a^{\dagger}_i$ ($a_i$) is the phonon creation (destruction) operator and $\omega_0$ the quantum of vibrational energy per site. The quantity $g_{ssh} = \alpha_{ssh}/\sqrt{2M\omega_0^3}$ is the SSH coupling that is mainly discussed in references [13,16], while $g_{hol} = \alpha_{hol}/\sqrt{2M\omega_0^3}$ is the Holstein local electron-phonon coupling. We use units such that the lattice spacing $a = 1$ and $\hbar = 1$.

## 3 Adiabatic limit

The adiabatic regime of the model is obtained in the limit of infinite ionic mass $M \to \infty$ keeping the spring constant and the el-ph couplings finite in the Hamiltonian (4). This assumption implies the neglecting of the quantum lattice fluctuations, so the lattice displacements become classical fields. In order to investigate the electronic features of the system, we need to fix the optimal lattice configuration. This is calculated by minimizing the ground state energy with respect to the lattice displacements. From equation (4) we obtain

$$E\left(\{x_k\}\right) = \left\langle -t \sum_i \left( c^{\dagger}_i c_{i+1} + c^{\dagger}_{i+1} c_i \right) + \alpha_{ssh} \sum_i \left( c^{\dagger}_i c_{i+1} + c^{\dagger}_{i+1} c_i \right) (x_{i+1} - x_i) + \alpha_{hol} \sum_i x_i c^{\dagger}_i c_i \right\rangle + \sum_i \frac{1}{2} K x_i^2, \quad (8)$$

where the ground state total energy $E(\{x_k\})$ has been written as the sum of the electronic energy in the lattice displacement classical fields $x_i$ and the energy of the fields $x_i$ themselves. In order to evaluate the mean value, we diagonalize the corresponding electronic Hamiltonian at any fixed configuration of the lattice displacements up to 40 sites. This allows us to calculate the phase diagram $\lambda_{ssh} = \alpha_{ssh}^2/4Kt = g_{ssh}^2/2\tilde{t}$ vs. $\lambda_{hol} = \alpha_{hol}^2/4Kt = g_{hol}^2/2\tilde{t}$, with $\tilde{t} = t/\omega_0$.

In the adiabatic regime of the SSH model ($\alpha_{hol} = 0$), the numerical analysis shows two solutions: the first characteristic of a free particle with vanishing deformations, the latter corresponding to a self-trapped state. However, this last solution has to be discarded since it is well known that the SSH model with optical phonons exhibits an unphysical region due to the pathological sign change of the next-nearest-neighbor hopping [13,16]. Figure 1 shows that in the SSH case the unphysical regions starts from $\lambda_{ssh} \geq 0.25$ [16]. In the adiabatic regime of the Holstein model ($\alpha_{ssh} = 0$), the total energy (8) always has a minimum corresponding to a self-trapped state. As discussed in reference [18], the radius of the localized state undergoes a smooth transition from large to small sizes and it is restricted to a lattice constant starting from values of $\lambda$ near to the unity. Here we assume that the localization occurs when the particle probability of being on the most deformed site is greater than 0.8 (in Fig. 1 the transition line to Holstein-like localization is dashed).

The case when both the couplings are present is very interesting. Indeed, the increase of the Holstein coupling enlarges the unphysical region caused by the SSH interaction, and, for large values of $\lambda_{hol}$, the critical values of $\lambda_{ssh}$ giving the unphysical behavior show a marked decrease. On the other hand, the SSH coupling favors the on-site Holstein-like localization and induces a non negligible electron probability also on the nearest-neighbor of the most deformed site. We notice that for finite values

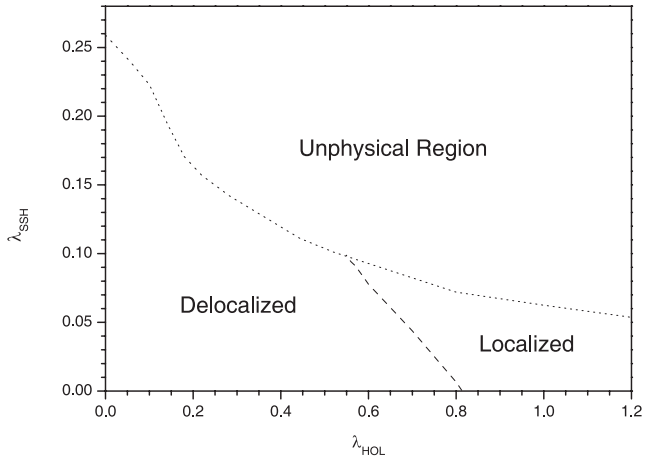


**Fig. 1.** Phase diagram of the system in the adiabatic regime for a chain of 40 sites. The localized region is determined by imposing that the particle probability of being on the most deformed site is greater than 0.8.

of the el-ph coupling constants the electronic wave function always develops a peak on the nearest-neighbor of the most deformed site, whose height depends on the values of the couplings in a non linear way. Such a feature prevents particle probability of becoming one on the most deformed site. Actually, we find that with the assumption made above by increasing $\lambda_{ssh}$ the localization is reached for smaller values of $\lambda_{hol}$. A different choice for the localization criteria can modify the shape of the transition line without changing this general trend. Therefore, there is a cooperative effect in influencing the properties of the electron obtained in the separate SSH and Holstein models. Since the physical region of the model is actually restricted to the weak coupling regime, in the next section we focus on it and use the perturbative approach to characterize the onset of the polaronic crossover.

## 4 Perturbation theory

The lowest-order perturbative approach has proved a remarkable useful tool in understanding the el-ph physics providing valuable indications on the beginning of the polaronic crossover [11,16]. In this paper we treat the el-ph interaction term $H_{int}$ as the perturbation and therefore we can explore both the adiabatic and the antiadiabatic regime considering small values of the el-ph couplings: $g_{ssh}, g_{hol} \ll min(\tilde{t}, 1)$. After transforming the phonon and the electron operators, one gets the following Hamiltonian in the momentum space

$$\hat{H} = \sum_k \varepsilon(k) c_k^\dagger c_k + \omega_0 \sum_q a_q^\dagger a_q + \hat{H}_{int} \tag{9}$$

where

$$\hat{H}_{int} = \frac{1}{\sqrt{N}} \sum_k g(k, k+q) c_{k+q}^\dagger c_k (a_{-q}^\dagger + a_q) + \frac{g_{hol}}{\sqrt{N}} \sum_k c_{k+q}^\dagger c_k (a_{-q}^\dagger + a_q), \tag{10}$$

with $\varepsilon(k) = -2t\cos(k)$ the bare electron band, $g(k, k+q) = -2ig_{ssh}\omega_0[\sin(k) - \sin(k+q)]$ the SSH vertex, and $N$ the total number of the lattice sites. It is straightforward to note that the coupling of the lattice distortion to the covalent bond $(c_i^\dagger c_{i+1} + c_{i+1}^\dagger c_i)$ arises a non-trivial momentum dependent vertex which competes with the Holstein one. Furthermore the SSH vertex vanishes as the transferred phononic momentum q is zero. In the next subsections we will show the different features induced by the two kinds of el-ph interactions on the spectral weight, the renormalized mass and the band structure.

In order to find the new energy and lifetime of the electron interacting with phonons as in (6), we need to evaluate the real and imaginary parts of the self-energy, which at the lowest perturbative order reads:

$$\Sigma(k, \omega) = \int_{-\pi}^{\pi} \frac{dq}{2\pi} \frac{|g(k+q, k)|^2}{\omega - \omega_0 - \varepsilon(k+q) + i\delta} + \int_{\pi}^{\pi} \frac{dq}{2\pi} \frac{g_{hol}^2 \omega_0^2}{\omega - \omega_0 - \varepsilon(k+q) + i\delta}. \tag{11}$$

The first and the second term of the right side of equation (11) define $\Sigma_{ssh}$ and $\Sigma_{hol}$, respectively. Carrying out the phonon momentum integration, one gets

$$\Re\Sigma_{ssh}(k, \omega) = -4g_{ssh}^2\omega_0 \left[ \frac{1-\tilde{\omega}}{4\tilde{t}^2} + \frac{\sin^2(k)}{\sqrt{1+\tilde{\omega}^2 - 2\tilde{\omega} - 4\tilde{t}^2}} - \frac{\sqrt{1+\tilde{\omega}^2 - 2\tilde{\omega} - 4\tilde{t}^2}}{4\tilde{t}^2} \right], \tag{12}$$

$$\Re\Sigma_{hol}(\omega) = -\frac{g_{hol}^2\omega_0}{\sqrt{1+\tilde{\omega}^2 - 2\tilde{\omega} - 4\tilde{t}^2}}, \tag{13}$$

$$\Im\Sigma_{ssh}(k, \omega) = -4g_{ssh}^2\omega_0 \left[ \frac{\sin^2(k)}{\sqrt{1+\tilde{\omega}^2 - 2\tilde{\omega} - 4\tilde{t}^2}} + \frac{\sqrt{1+\tilde{\omega}^2 - 2\tilde{\omega} - 4\tilde{t}^2}}{4\tilde{t}^2} - \frac{\sin(k)}{\tilde{t}} \right], \tag{14}$$

$$\Im\Sigma_{hol}(\omega) = -\frac{g_{hol}^2\omega_0}{\sqrt{1+\tilde{\omega}^2 - 2\tilde{\omega} - 4\tilde{t}^2}}, \tag{15}$$

for $(1-\tilde{\omega}) > 2\tilde{t}$, with $\tilde{\omega} = \omega/\omega_0$. As one can see, the interactions with phonons lower the energy levels of the electron (see below). Moreover, the value of the self-energy as a function of $\omega$ has a singularity as $\omega \to \omega_0 - 2t$, i.e. $k \to k_c = \arccos(1 - 1/2\tilde{t})$ within the on shell approximation. The nature of this singularity is determined by the behavior of the function inside the integral for $q$ near to $k_c$, as discussed in [19]. Since for $k \to k_c$ the inverse quasiparticle lifetime $\Im\Sigma$ diverges, there is no quasiparticle close to the threshold, as for the Holstein case.

### 4.1 Spectral weight and effective mass

An insight in the polaron formation is provided by the behavior of the spectral weight and the effective mass. Actually, the polaron crossover is expected to be associated with a reduction of the spectral weight and an enhancement of the charge carrier mass. The spectral weight and the renormalized mass are defined as

$$Z(k=0) = \frac{1}{(1 - \partial \Re\Sigma(k,\omega)/\partial\omega|_{\omega=-2t,k=0})}, \tag{16}$$

$$\frac{m_{eff}}{m} = \frac{1}{Z(k=0)(1+\partial \Re\Sigma_{ssh}(k,\omega)/\partial\varepsilon(k)|_{\omega=-2t,k=0})}, \tag{17}$$

where $m$ is the bare band mass. It is worthwhile noticing that, since the Holstein contribution to the self-energy is momentum independent, if $g_{ssh} = 0$ then $m/m_{eff} = Z(0)$. Such a feature of the Holstein coupling strictly links the reduction of the coherence of the electron to its localization in any coupling regime [20]. The SSH non-local coupling breaks down this picture introducing a momentum dependence in the self-energy expression. From the equations above, one gets

$$Z(k=0) = \left(1 + \frac{g_{ssh}^2}{\tilde{t}^2}\left[\frac{(1+2\tilde{t})}{\sqrt{1+4\tilde{t}}} - 1\right] + g_{hol}^2 \frac{(1+2\tilde{t})}{(1+4\tilde{t})^{3/2}}\right)^{-1}, \tag{18}$$

$$\frac{m_{eff}}{m} = 1 + \frac{g_{ssh}^2}{2\tilde{t}}\left[\frac{8}{\sqrt{1+4\tilde{t}}} + \frac{2}{\tilde{t}}\left(\frac{2\tilde{t}+1}{\sqrt{1+4\tilde{t}}} - 1\right)\right] + g_{hol}^2 \frac{(1+2\tilde{t})}{(1+4\tilde{t})^{3/2}}. \tag{19}$$

We show the spectral weight $Z(k=0)$ and the inverse ratio $m/m_{eff}$ for $\tilde{t} = 1$ as functions of $g_{hol}$ and $g_{ssh}$ in the left and right panel of the Figure 2, respectively. As expected, an increase of the el-ph coupling strength yields a reduction of the spectral weight and an enhancement of the effective mass. However the mass renormalization effects are much more sensitive to the coupling parameter $g_{ssh}$, pointing out that the SSH mechanism of localization can be more effective than the Holstein one.

In Figure 3 we plot $Z(k=0)$ and $m_{eff}/m$ as functions of the inverse adiabaticity ratio $\tilde{t}$. By increasing $\tilde{t}$, the renormalization factor $Z(k=0)$ asymptotically goes to 1 and the effective mass decreases towards the band mass value. It is interesting to note that the reduction of $Z(k=0)$ due to the SSH contribution is more important than the Holstein one for $\tilde{t} < 2$, while the SSH contribution to the mass enhancement is larger than the Holstein one for all values of $\tilde{t}$.

The correlation between the behaviors of the spectral weight and the effective mass established by equation (17) is quantified in Figure 4, where we plot the ratio $Z(k=0)/(m/m_{eff})$ versus $\tilde{t}$ for different values of the coupling constant $g_{ssh}$. The curves of Figure 4 clearly show that this ratio is always greater than 1, pointing out that the non-local interaction term is more effective for the mass enhancement rather than for the reduction of the spectral weight. In particular an increase of $g_{ssh}$ and a decrease of $\tilde{t}$ produce larger values of the ratio supporting the tendency towards localization. We stress that the opposite occurs for long-range el-ph "density-displacement" Fröhlich interactions. Within the weak-coupling perturbative approach, in the continuum case it is well known that the ratio $Z(0)/(m/m_{eff})$ is less than 1, being $Z(0)/(m/m_{eff}) \simeq (1-\alpha/2)/((1-\alpha/6)$, with $\alpha$ the dimensionless el-ph coupling constant [21]. Recently values of the ratio less than 1 are also found for the extension of the Fröhlich polaron model to a discrete ionic lattice [22,23]. In such a case, in the adiabatic regime a range of values of the el-ph coupling is found where the ground state is well described by a particle with a weakly

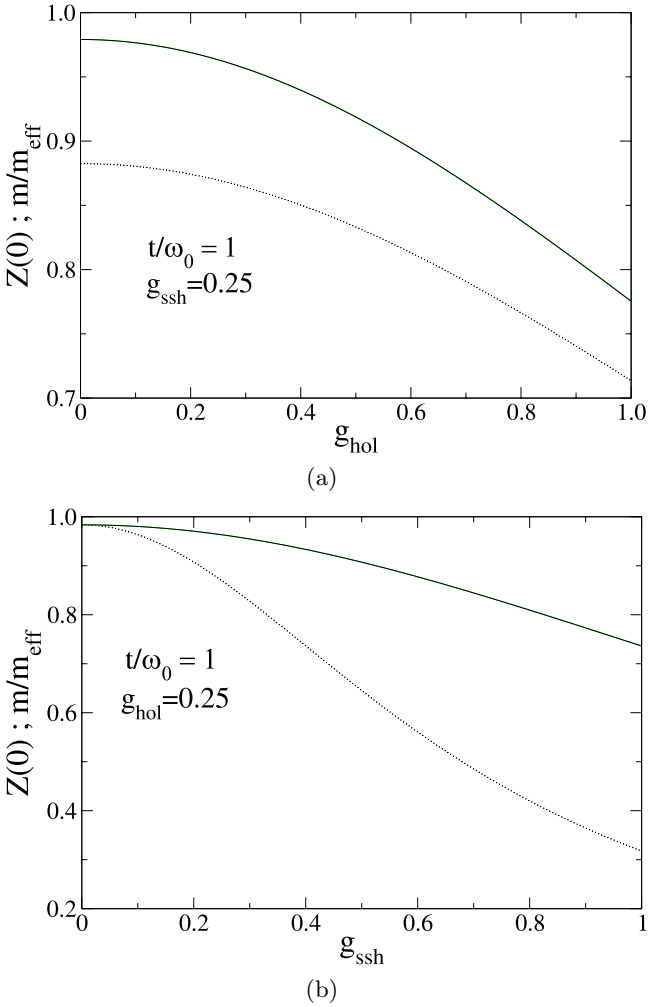


**Fig. 2.** (a) Spectral weight $Z(0)$ (solid line) and polaron effective mass inverse ratio $m/m_{eff}$ (dashed line) as functions of the Holstein coupling $g_{hol}$ for a fixed value of the SSH coupling $g_{ssh}$. (b) $Z(0)$ (solid line) and $m/m_{eff}$ (dashed line) vs. SSH coupling $g_{ssh}$ for a fixed value of the Holstein coupling $g_{hol}$.

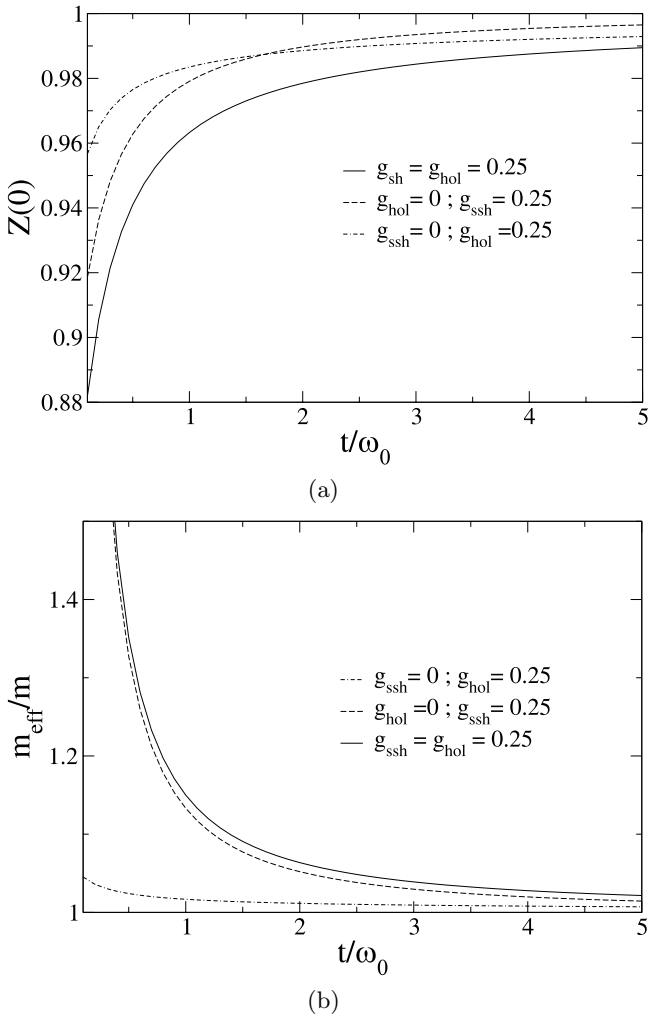


**Fig. 3.** (a) Spectral weight $Z(0)$ (solid line) vs. $\tilde{t}$ for $g_{ssh} = g_{hol} = 0.25$. The dashed and the dot-dashed lines show the SSH contribution ($g_{hol} = 0$) and the Holstein contribution ($g_{ssh} = 0$), respectively. (b) Effective mass respect band mass (solid line) vs. $\tilde{t}$ for $g_{ssh} = g_{hol} = 0.25$. The dashed and the dot-dashed lines show the SSH contribution ($g_{hol} = 0$) and the Holstein contribution ($g_{ssh} = 0$), respectively.

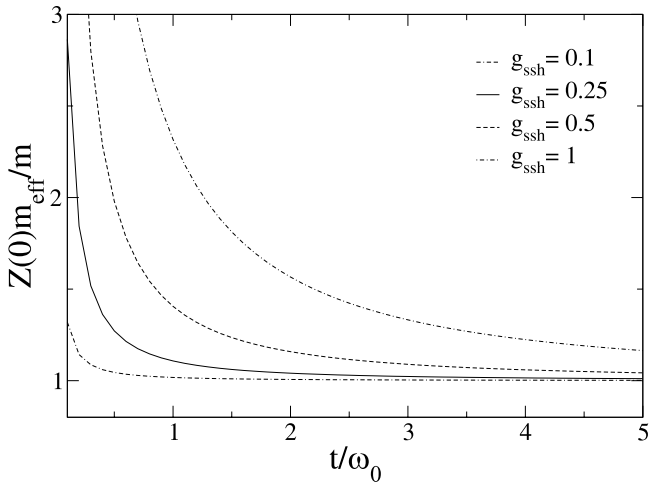


**Fig. 4.** Ratio $Z/(m/m_{eff})$ at $k = 0$ as function of $\tilde{t}$ for four different values of $g_{ssh}$ and $g_{hol} = 0.25$.

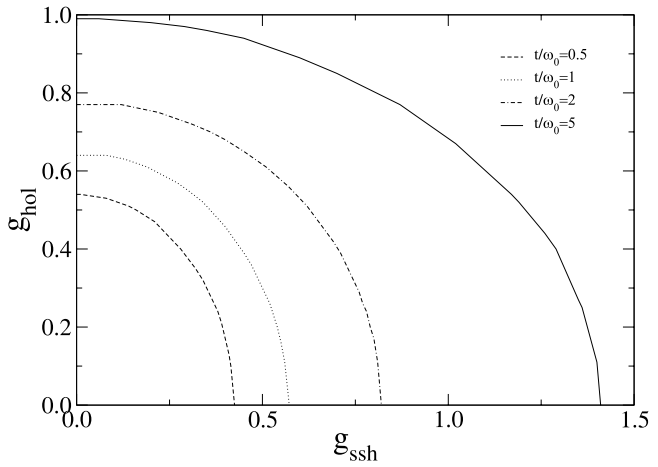


**Fig. 5.** Phase-diagram $g_{hol}$ versus $g_{ssh}$ for a single charge carrier in a discrete chain. The crossover lines correspond to different values of $\tilde{t}$ and divide the parameter space in the two regions $Z(0) > 0.9$ and $Z(0) < 0.9$.

renormalized mass and a spectral weight much smaller than unity [23]. Therefore the Fröhlich-like non-local interaction favors the transfer of the spectral weight at higher energies with increasing the coupling constant. On the contrary the SSH coupling mainly supplies an enhancement of the effective mass.

### 4.2 Phase diagram

We conclude our analysis at $k = 0$ calculating the phase diagram of Figure 5. The crossover lines are defined as the set of the coupling values for which $Z(0)$ is equal to 0.9. Below the curves, one has $Z(0) > 0.9$, so electrons are expected to be the natural quasi-particles of the system in which the el-ph interactions are weak [23]. Above the lines the spectral weight reduction signals that electrons are no more good quasiparticles and indicates the onset of polaronic features, confirmed by the effective mass calculation. As shown in the phase-diagram, by increasing $\tilde{t}$, the crossover region shifts towards larger values of the el-ph couplings, where the application of a low order perturbative theory starts to be questionable. However we wish to stress that the simultaneous presence of the non-local SSH coupling allows smaller values of the local Holstein coupling constant to drag the system in the crossover region.

### 4.3 Energy bands

The energy bands renormalized by the el-ph couplings are obtained evaluating the real part of the self-energy on the energy-shell:

$$E(k) = \varepsilon(k) + \Re\Sigma_{ssh}(k, \varepsilon(k)) + \Re\Sigma_{hol}(\varepsilon(k)). \qquad (20)$$

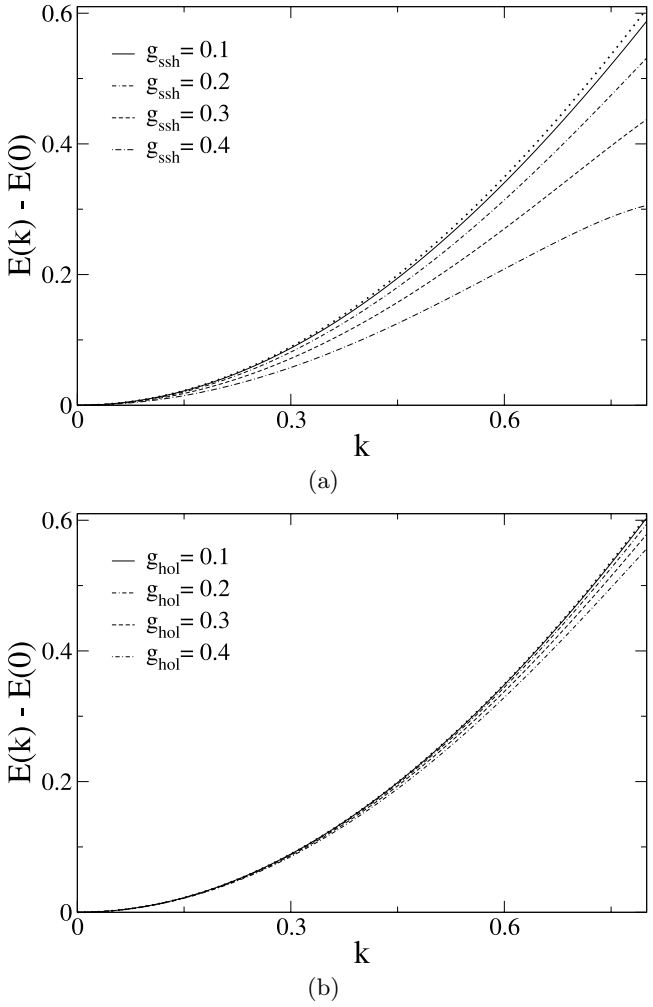


**Fig. 6.** (a) SSH band structures for different values of $g_{ssh}$ and $\tilde{t} = 1$. (b) Holstein band structures for different values of $g_{hol}$ and $\tilde{t} = 1$. The free band (dotted line) is shown for comparison.

As stressed above, it is well-known that the perturbative approach breaks down as the energy measured from the bottom of the band equals the phonon frequency $\omega_0$, i.e. at $k = k_c$. Actually, for $|k| > k_c$, the particle becomes unstable to optical phonon emission and the dispersion curve bends over and becomes horizontal [24,25]. Therefore, for $\tilde{t} > 1/4$ we restrict our analysis to the region $|k| < k_c$.

First, we compare the SSH ($g_{hol} = 0$) and the Holstein ($g_{ssh} = 0$) contributions to the band structure of the model and plot them for $\tilde{t} = 1$ in the left and right panel of Figure 6, respectively. As one can see, the SSH contribution modifies the shape of the energy band. Indeed, larger values of $g_{ssh}$ induce stronger deviations from the free band structure at each fixed wave-vector number. Moreover the distortion of the curvature increases moving away from the bottom of the band. On the contrary, the band structure essentially stays cosine-like on varying the Holstein coupling. When both the el-ph interactions are effective in the investigated weak-coupling regime we find that the band shape is dominated by the SSH contribution over almost the whole Brillouin zone. Thus, differently from the Holstein model where distortions of the energy bands are found only in the intermediate regime of the local coupling, the simultaneous manifestation of weak local and non-local el-ph interactions is responsible for nonsinusoidal dependence on $k$ of the energy bands, reflecting polaron structure. For $\tilde{t} < 1/4$ the largest deviations from the bare electron band are obtained at the zone-edge where both the contributions are relevant, yielding a non negligible bandwith reduction.

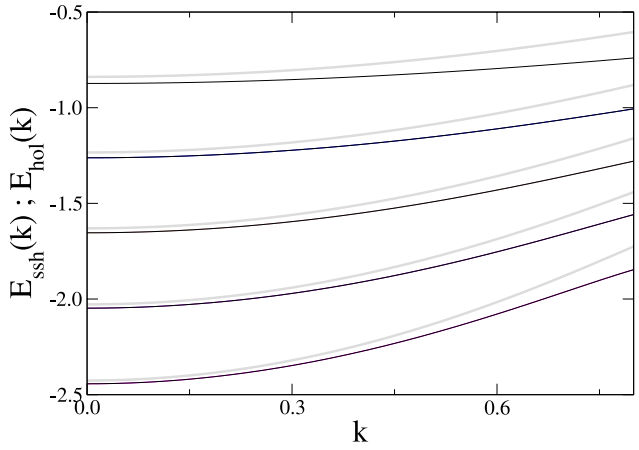


**Fig. 7.** Band structures for different values of the inverse adiabatic ratio $\tilde{t}$. From the top to the bottom $\tilde{t} = 0.4, 0.6, 0.8, 1.0, 1.2$. Solid grey lines show the Holstein contribution ($g_{ssh} = 0$ and $g_{hol} = 0.25$); solid black lines show the SSH contribution ($g_{hol} = 0$ and $g_{ssh} = 0.25$).

Finally, we determine how the band structure is affected by the degree of adiabaticity of the system. In Figure 7 we plot the SSH ($g_{hol} = 0$) and the Holstein ($g_{ssh} = 0$) contributions for several values of $\tilde{t}$. As shown, the flattening of the curves with decreasing $\tilde{t}$ is more pronounced for the non-local contribution. Moreover we observe that for $k$ values close to the bottom of the band ($k = 0$) the difference between the two energy contributions increases by decreasing $\tilde{t}$. Thus, moving towards the antiadiabatic regime, the SSH contribution is more and more effective than the Holstein one to determine the low energy states of the system.

## 5 Conclusions

We investigated polaron features in a discrete chain taking into account both the local Holstein and the non-local SSH coupling. In particular, we studied the adiabatic limit of the model and characterized the onset of the polaronic crossover analyzing the behavior of the spectral weight and the effective mass. Both in the adiabatic and antiadiabatic regime we found that the non-local el-ph interaction provides a large mass enhancement which is no more simply related to the reduction of the spectral weight a $k = 0$, like in the Holstein model. In particular we showed that the non-local SSH coupling is more effective for the mass enhancement rather than for the reduction of the spectral

weight, contrarily to what happens for long-range Fröhlich interactions. Moreover we calculated the phase diagram $g_{hol}$ vs. $g_{ssh}$ and showed that the simultaneous action of the two el-ph interactions more easily drives the system in the crossover region. Finally, in order to quantify the effects of the different el-ph couplings on the polaron bands, we performed an analysis of the band structures varying the adiabaticity parameter and the el-ph coupling constants. We emphasized that the curvature induced by the considered one-phonon scattering processes changes qualitatively the shape of the bare electron band.

In order to overcome the limitations of the weak-coupling regime it is possible to study the system introducing a variational wave function that includes the features of both the local and non-local coupling. This can be achieved by extending the variational approach of a recent paper [13]. Work in this direction is in progress.

## References


1. J.T. Devreese, *Polarons*, in: *Encyclopedia of Applied Physics*, Vol. 14, edited by G.L. Trigg (VCH Publishers, New York, 1996), p. 383
2. A.S. Alexandrov, N.F. Mott, *Polarons and Bipolarons* (World Scientific, Singapore, 1995); A.S. Alexandrov *Theory of superconductivity: from weak to strong coupling* (IOP Publishing, 2003)
3. J.M. De Teresa, M.R. Ibarra, P.A. Algarabel, C. Ritter, C. Marquina, J. Blasco, J. Garcia, A. del Moral, Z. Arnold, Nature **386**, 256 (1997); A.J. Millis, Nature **392**, 147 (1998); M.B. Salamon, M. Jaime, Rev. Mod. Phys. **73**, 583 (2001)
4. M. Matus, H. Kuzmany, E. Sohmen, Phys. Rev. Lett. **68**, 2822 (1992); K. Harigaya, Phys. Rev. B **45**, 13676 (1992); B. Friedman, Phys. Rev. B **45**, 1454 (1992); W.M. You, C.L. Wang, F.C. Zhang, Z.B. Su, Phys. Rev. B **47**, 4765 (1993)
5. M. Verissimo-Alves, R.B. Capaz, B. Koiller, E. Artacho, H. Chacham, Phys. Rev. Lett. **86**, 3372 (2001); E. Piegari, V. Cataudella, V. Marigliano Ramaglia, G. Iadonisi Phys. Rev. Lett. **89**, 049701 (2002); L.M. Woods, G.D. Mahan, Phys. Rev. B **61**, 10651 (2000); H. Suzura, T. Ando, Phys. Rev. B **65**, 235412 (2002)
6. Yu N. Gartstein, A.A. Zakhidov, R.H. Baughman, Phys. Rev. Lett. **89**, 045503 (2002)
7. Guo-Meng-Zhao, M.B. Hunt, H. Keller, K.A. Muller, Nature **385**, 236 (1997); A. Lanzara, P.V. Bogdanov, X.J. Zhou, S.A. Kellar, D.L. Feng, E.D. Lu, T. Yoshida, H. Eisaki, A. Fujimori, K. Kishio, J.-I. Shimoyama, T. Noda, S. Uchida, Z. Hussain, Z.-X. Shen, Nature **412**, 510 (2001); R.J. McQueeney, J.L. Sarrao, P.G. Pagliuso, P.W. Stephens, R. Osborn, Phys. Rev. Lett. **87**, 77001 (2001)
8. S.S. Alexandre, E. Artacho, J.M. Soler, M. Chacham, Phys. Rev. Lett. **91**, 108105 (2003)
9. Y. Lu, *Solitons and Polarons in Conducting Polymers* (World Scientific, Singapore, 1988)
10. A. La Magna, R. Pucci, Phys. Rev. B **55**, 6296 (1997)
11. M. Zoli, Phys. Rev. B **66**, 012303 (2002); M. Zoli, Phys. Rev. B **67**, 195102 (2003); M. Zoli, Solid State Comm. **122**, 531 (2002)
12. Chun-Min Chang, A.H.C. Neto, A.R. Bishop, Chem. Phys. **303**, 189 (2004)
13. C.A. Perroni, E. Piegari, M. Capone, V. Cataudella, Phys. Rev. B **69**, 174301 (2004)
14. T. Holstein, Ann. Phys. **8**, 325 (1959); T. Holstein, Ann. Phys. **8**, 343 (1959)
15. W.P. Su, J.R. Schrieffer, A.J. Heeger, Phys. Rev. Lett. **42**, 1698 (1979); W.P. Su, J.R. Schrieffer, A.J. Heeger, Phys. Rev. B **22**, 2099 (1980)
16. M. Capone, W. Stephan, M. Grilli, Phys. Rev. B **56**, 4484 (1997)
17. We recall that at zero temperature the imaginary part of the self-energy vanishes as the energy $\omega$ measured from the bottom of the band is less than the phonon frequency. Therefore, in order to study the properties of the ground state $k = 0$, we have to consider only the real part of the self-energy
18. V.V. Kabanov, O. Yu Mashtakov, Phys. Rev. B **47**, 6060 (1993)
19. Y.B. Levinson, E.I. Rashba, Rep. Progr. Phys. **36**, 1499 (1973)
20. H. Fehske, J. Loos, G. Wellein, Phys. Rev. B **61**, 8016 (2000)
21. G.D. Mahan, *Many Particle Physics* (Plenum Press, New York, 1981)
22. A.S. Alexandrov, P.E. Kornilovitch, Phys. Rev. Lett. **82**, 807 (1999); A.S. Alexandrov, Phys. Rev. B **61**, 12315 (2000); A.S. Alexandrov, C. Srincheewin, Europhys. Lett. **51**, 188 (2000)
23. C.A. Perroni, V. Cataudella, G. De Filippis, J. Phys.: Condens. Matter **16**, 1593 (2004)
24. A.H. Romero, D.W. Brown, K. Lindenberg, Phys. Rev. B **59**, 13728 (1999)
25. V. Cataudella, G. De Filippis, G. Iadonisi, Phys. Rev. B **60**, 15163 (1999)